Supporting information

For

Hierarchical molybdenum-doped NiCoP@carbon microspheres: A highly-efficient electrocatalyst for hydrogen evolution reaction

Changhai Liu[a], Yanhua Yao[a], Lei Sun[a], Linlin Luo[a], Wenchang Wang[b], Zhidong Chen[b,*]

[a]*School of Materials Science and Engineering, Jiangsu Collaborative Innovation Center of Photovoltaic Science and Engineering, Changzhou University, Changzhou, 213164, Jiangsu, China.*

[b]*School of Petrochemical Engineering, Changzhou University, Changzhou, 213164, Jiangsu, China E-mail: zdchen@cczu.edu.cn*

Experimental section

Materials

Cobalt nitrate hexahydrate ($Co(NO_3)_2 \cdot 6H_2O$), nickel nitrate ($Ni(NO_3)_2 \cdot 6H_2O$), glycerol, isopropanol, phosphomolybdic acid and ethanol were purchased from Aladdin Ltd. (Shanghai, China). Nafion (5 wt%) was purchased from Sigma-Aldrich. All the reagents were used as received without further purification. The water, used throughout all experiments,was distilled water.

Preparation of NiCo-glycerate precursor

Firstly, 100 mg of cobalt nitrate hexahydrate, 50 mg of nickel nitrate hexahydrate and 12 ml of glycerol were added in 50 ml of isopropanol under vigorous stirring for 15 min to form a mixed solution. Then, the above mixture was transferred into a solvothermal reactor and heated under 180°C for 10 h. The obtained pink NiCo-glycerol precursor was washed with ethanol several times and dried under vacuum at 60°C overnight. Similarly, Co-glycerol precursor and Ni-glycerol precursor were prepared with 150 mg of cobalt nitrate hexahydrate and 150 mg of nickel nitrate hexahydrate respectively.

Synthesis of MNiCoP@C nanospheres

Typically, 50 mg of as-prepared NiCo-glycerol precursor and phosphomolybdic acid were dispersed in 60 ml of ethanol at a magnetic stirring for 30 min (Phosphomolybdic acid accounts for 10% of the mass of precursor). After that, the above suspension was

transformed into a solvothermal reactor and kept at 160°C for 6 h. After cooling naturally, the brown precipitation was centrifuged and washed with ethanol, and then, dried at 60°C under vacuum overnight (noted as MNiCoP@C-10). The preparations of Co-Mo nanospheres and Ni-Mo nanospheres were similar to the above process. Finally, to improve the crystallinity of the final dark powder, a thermal annealing treatment was carried out at 350°C for 2 h at a heating rate of 2 °C min^{-1} under a nitrogen atmosphere. As references, the different reactant mass of precursor (5%、15%) were also be explored, the resultants were denoted as MNiCoP@C-5 and MNiCoP@C-15, respectively.

Characterizations

X-ray diffraction (XRD) patterns were collected on a powder X-ray diffractometer at 40 kV and 15 mA using Cu-Kα radiation (λ=1.54056 Å, PANalytical X'Pert Powder diffractimeter). The Raman spectra were carried out on LabRAM HR Evolution spectrometer (HORIBA Jobin Yvon) with an excitation wavelength of 532 nm. Transmission electron microscopy (TEM) and high resolution TEM (HRTEM) images were obtained on a JEOL JEM-2100F microscope at 200 kV. Scanning electron microscopy (SEM) images were recorded on the FEI Quanta 450 at high vacuum with an accelerating voltage of 10 kV.The field emission scanning electron microscopy (FESEM) were observed under a SUPRA-55 electron microscopy. X-ray photoelectron spectra (XPS) spectrometer equipped with an Al Ka source (1486.6 eV).

Electrochemical characterization

HER measurements were performed with a three-electrode glass cell. The data were recorded using a CHI 660E bipotentiostat (CH Instruments, Inc., USA). The reference electrode was Ag/AgCl in saturated KCl solution (4 mol/L) and the counter electrode was a graphite rod. The current density was normalized to the geometrical surface area and the measured potentials vs. Ag/AgCl were converted to a reversible hydrogen electrode (RHE) scale according to the Nernst equation (E_{RHE} =$E_{Ag/Ag/Cl}$ +0.059*pH+0.197).The polarization curves were recorded with the scan rate of 2 mV/s. The working electrodes were scanned for several times until the signals were stabilized, and then the data for polarization curves were collected, corrected for the iR contribution within the cell. The onset potentials were determined based on the beginning of the linear region in Tafel plots.

Electrochemical impedance spectroscopy (EIS) was measured via adopting symmetric cells with the same electrolyte in solar cells. The corresponding frequency ranged from 0.1 Hz to 100 k Hz with adisturbed amplitude of 5 mV/s. The electrical double layer capacitor (C_{dl}) and surface roughness factor (R_f) of the as-synthesized materials were measured from double-layer charging curves using cyclic voltammograms (CVs) in a small potential range of 0.4-0.5 V vs. RHE.Working electrodes were scanned for several potential cycles until the signals were stabilized, and then the CV data were collected.The plot of current density (at 0.45 V vs. RHE) against scan rate has a linear relationship and its slope is the double layer capacitance(C_{dl}). The R_f was calculated by dividing C_{dl} by the capacitance of ideal planar metal oxides (e.g. Co_3O_4) having smooth surface, normally taken to be 60 $\mu F\ cm^{-2}$.

Calculation of ESCA

Based on the linear fitting of Figure 4, we can derive its specific capacitance as follows:

$$C_{Ni-Co-Mo-10} = \frac{k}{2} \times \frac{1}{m} = \frac{54.1mF/cm^2}{2} \times \frac{1}{0.43mg/cm^2} = 62.9F/g$$

Where C is the specific capacitance of M1N0.5, k is the fitting slope, m is the catalyst areal loading.

Then, we can calculate its ESCA by assuming a standard value of 60 uF/cm²:

$$ECSA_{Ni-Co-Mo-10} = \frac{C}{60\mu F/cm^2} = \frac{62.9F/g}{60\mu F/cm^2} = 104.8m^2/g$$

As the calculation process of Ni-Co-Mo-10, we can get the C and ECSA of Ni-Co-Mo-5 , Ni-Co-Mo-15, CoMo, Ni-Mo and CoNi.

$$C_{Ni-Co-Mo-15} = \frac{k}{2} \times \frac{1}{m} = \frac{14.2mF/cm^2}{2} \times \frac{1}{0.43mg/cm^2} = 16.5F/g$$

$$ECSA_{Ni-Co-Mo-15} = \frac{C}{60\mu F/cm^2} = \frac{16.5F/g}{60\mu F/cm^2} = 27.5m^2/g$$

$$C_{Ni-Co-Mo-5} = \frac{k}{2} \times \frac{1}{m} = \frac{13.0mF/cm^2}{2} \times \frac{1}{0.43mg/cm^2} = 15.1F/g$$

$$ECSA_{Ni-Co-Mo-5} = \frac{C}{60\mu F/cm^2} = \frac{15.1F/g}{60\mu F/cm^2} = 25.2m^2/g$$

$$C_{CoMo} = \frac{k}{2} \times \frac{1}{m} = \frac{10.1mF/cm^2}{2} \times \frac{1}{0.43mg/cm^2} = 11.7F/g$$

$$ECSA_{CoMo} = \frac{C}{60\mu\,F\,/\,cm^2} = \frac{11.7F\,/\,g}{60\mu\,F\,/\,cm^2} = 19.5m^2\,/\,g$$

$$C_{NiMo} = \frac{k}{2} \times \frac{1}{m} = \frac{9.8mF\,/\,cm^2}{2} \times \frac{1}{0.43mg\,/\,cm^2} = 11.4F\,/\,g$$

$$ECSA_{NiMo} = \frac{C}{60\mu\,F\,/\,cm^2} = \frac{11.4F\,/\,g}{60\mu\,F\,/\,cm^2} = 18.9m^2\,/\,g$$

$$C_{CoNi} = \frac{k}{2} \times \frac{1}{m} = \frac{5.6mF\,/\,cm^2}{2} \times \frac{1}{0.43mg\,/\,cm^2} = 6.5F\,/\,g$$

$$ECSA_{CoNi} = \frac{C}{60\mu\,F\,/\,cm^2} = \frac{6.5F\,/\,g}{60\mu\,F\,/\,cm^2} = 10.8m^2\,/\,g$$
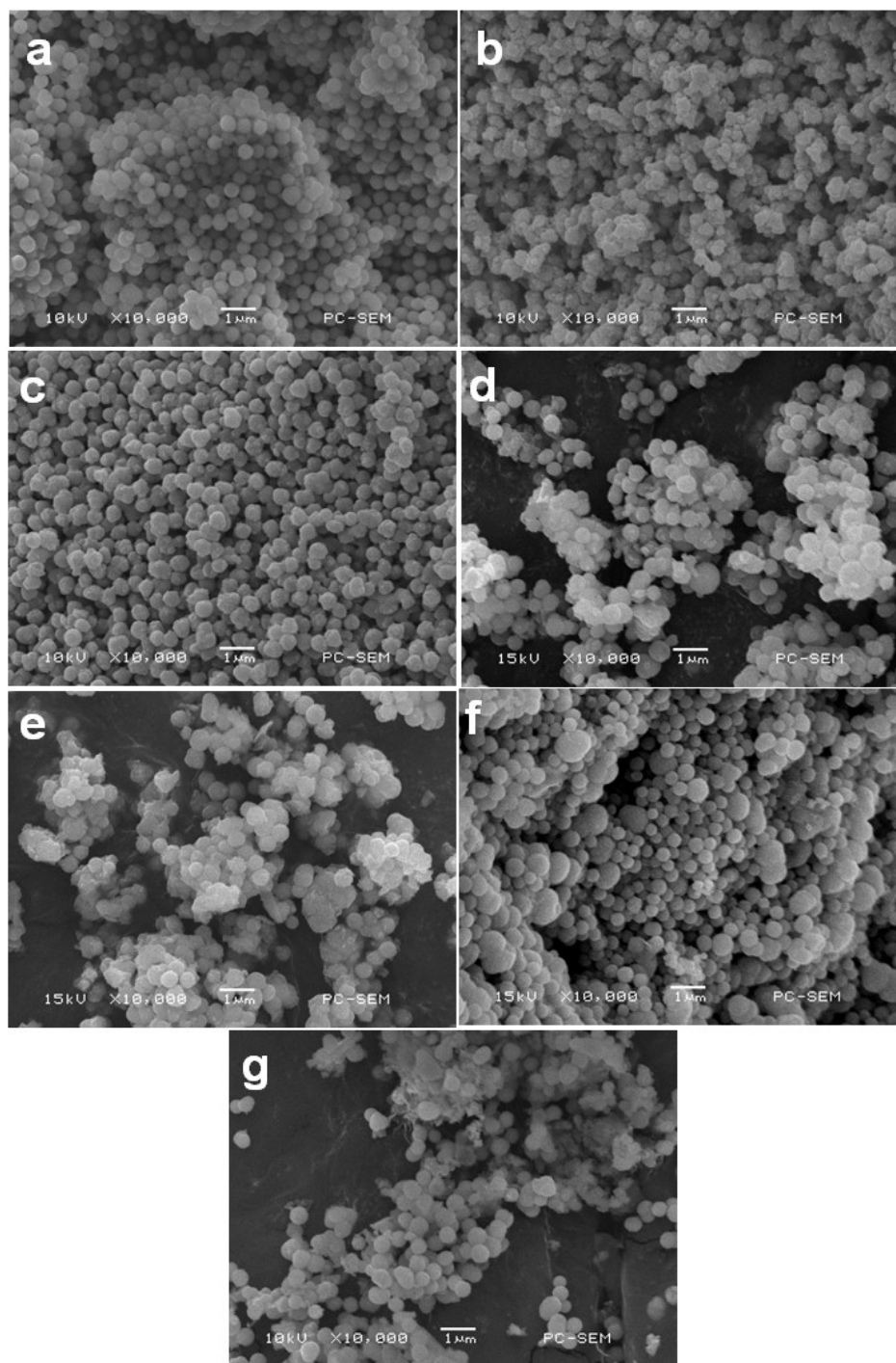
Figure S1 SEM images of (a) Co-GL, (b) Ni-GL, (c) NiCo-GL, (d) MCoP@C, (e) MNiP@C, (f) MNiCoP@C (5%) and (f) MNiCoP@C (15%) samples, respectively.
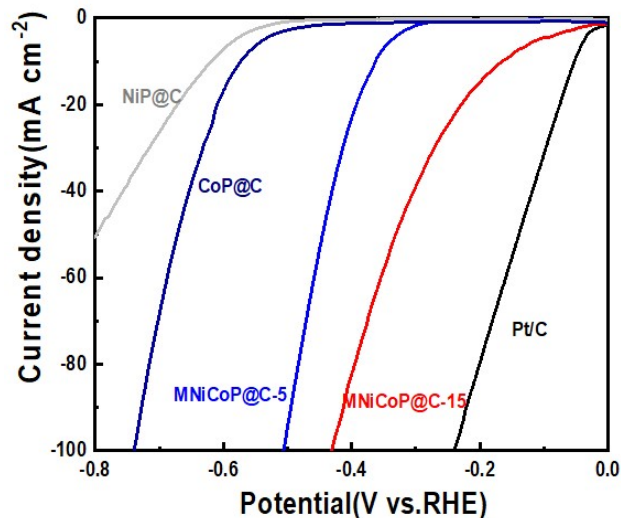
Figure S2 Polarization curves of Pt/C, MNiCoP@C-5, MNiCoP@C-15, CoP@C-5, and Ni@C respectively.

The LSV results in Figure S2 indicates the introduction of Mo species into catalysts can significantly decrease the overpotential. In addition, the MNiCoP@C-5 and MNiCoP@C-15 exhibited enhanced HER activity compared catalysts without Mo addition. Compared with MNiCoP@C-5 and MNiCoP@C-15 samples, the MNiCoP@C-10 exhibited the best HER activity, showing the lowest overpotential at 10 mA cm^{-2}.
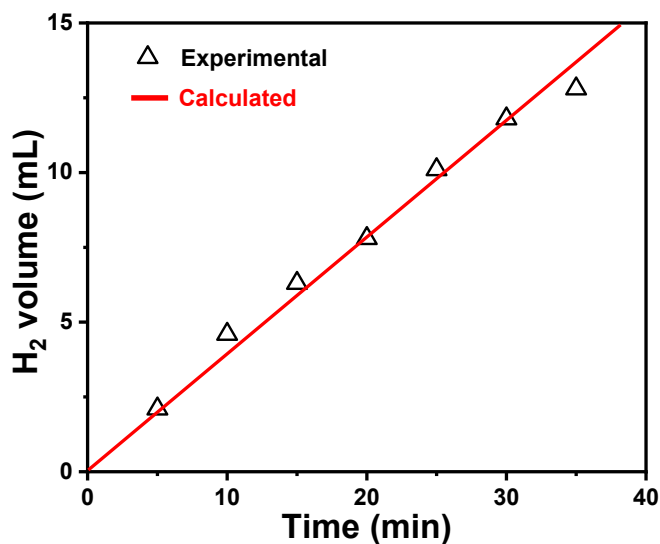

Figure S3 The amount of H_2 theoretically calculated and experimentally measured versus time of HER on MNiCoP@C-10 with a current of 60 mA.
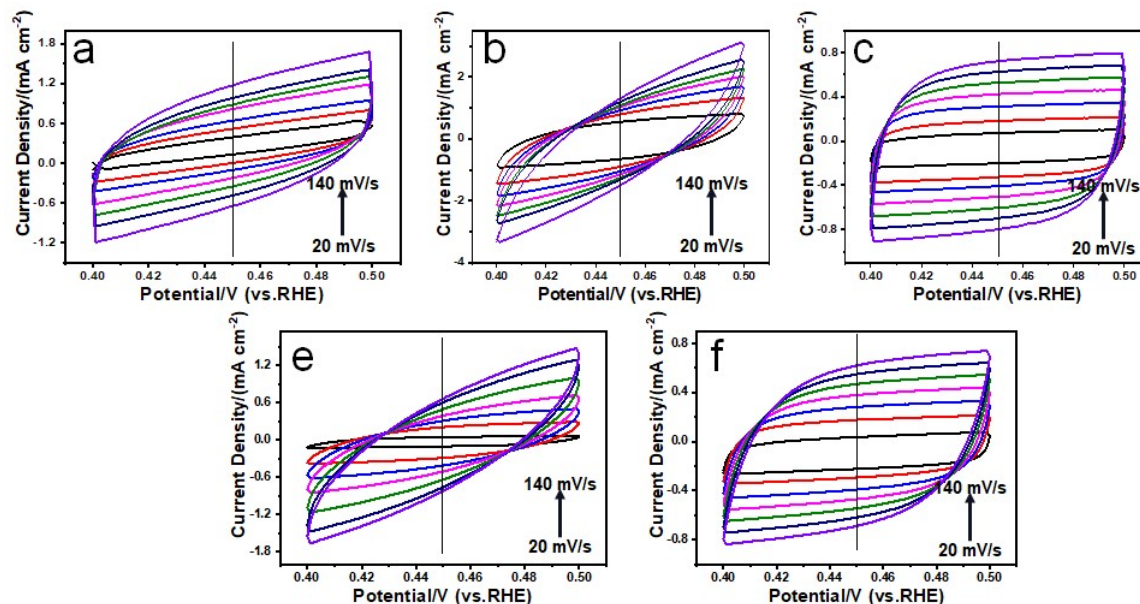
Figure S4 The current density with different scan rate of 20, 40, 60, 80, 100, 120, and 140 mV/s for (a) MNiCoP@C-5, (b) MNiCoP@C-15, (c) MNiCoP@C-10, (d) MCoP@C, and MNiP@C samples, respectively.

Table S1 The comparison of HER performance for different catalysts in literature

Samples	Loading	Electrolyte	Current Density	Overpotential(mV)	Tafel(mV/dec)	j_0 (mA cm^{-2})	Reference
Ni$_{0.5}$-Mo$_2$C/NC	0.43mg/cm^2	0.5M H$_2$SO$_4$	10	114	52.8	0.584	*In this work*
		1 M KOH	10	147	76.1	0.580	
MoNCs	0.23mg/cm^2	0.5M H$_2$SO$_4$	10	~ 200	60.6	0.0265	Nano-Micro Lett,2019, 11,45
MoS$_2$/Mo$_2$C	0.25mg/cm^2	0.5M H$_2$SO$_4$	10	~ 105	53	0.9	ACS Catal.(2017)7107312-7318
Mo$_2$C-carbon sphere	0.28mg/cm^2	0.5M H$_2$SO$_4$	10	~ 164	85	0.179	Chemistry A European Journal,2017,10947-10961
Mo$_2$N-Mo$_2$C/HGr-3	0.25mg/cm^2	0.5M H$_2$SO$_4$	10	~ 157	55	0.062	ACS Energy Lett., 2016, 1, 589-594
		1M KOH	10	~154	68	0.497	
Mo$_2$C/C	0.28mg/cm^2	0.5M H$_2$SO$_4$	10	~ 180	71	-	ACS Appl. Mater. Interfaces2017, 947, 41314-41322
		1M KOH	10	~125	72	-	
Mo$_2$C@C	0.35mg/cm^2	0.5M H$_2$SO$_4$	10	~ 110	83	-	Journal of Catalysis,2018, 9-19
		1M KOH	10	~60	70	-	
Mo$_2$C/CNT	0.57mg/cm^2	0.5M H$_2$SO$_4$	10	~ 112	53.6	-	Electrochimica Acta,2018, 192-200

Mo₂C/MoN /NG	0.57 mg/cm²	0.5M H₂SO₄	10	~ 78.82	39.3	-	Nano Res. (2018) 11: 4535
B,N:Mo2C/ BCN	-	1M KOH	10	~94	62	0.346	ACS Catal.2018,898296-8305
N,P-MoₓC NF	0.265mg /cm²	0.5M H₂SO₄	10	~ 107	65.1	0.25	ACS Appl. Mater. Interfaces201810171 4632-14640
Mo₂C-PPyF-1/1	0.5 mg/cm²	0.5 M H₂SO₄.	10	~177.5	59.6	0.0102	Electrochimica Acta,2018, 578-587
β-Mo₂C-C	0.35 mg/cm²	1 M KOH	10	~146	90	-	*International Journal of Hydrogen Energy ,2018, 21655-21664*
Mo₂C@C	0.28 mg/cm²	1 M KOH	10	~100	53	0.138	*International Journal of Hydrogen Energy,2019, 3702-3710*

Table S2 The exchange current for different samples in 1M KOH

Sample	Exchange current (J_0 mA/cm²)
MNiCoP@C-10	0.552
MNiCoP@C-15	0.345
MNiCoP@C-5	0.278
MCoP@C	0.140
MNiP@C	0.091
NiCo@C	0.063
Pt/C	0.757

Table S3 Z-fit equivalent circuit data of EIS results obtained in 1.0 M KOH

Sample	Rs (Ω) / Error (%)	Rct (Ω) / Error (%)	CPE (μF) / Error (%)
MNiCoP@C-10	10.45, 4.27	115.3, 3.40	58.3, 4.01
MNiCoP@C-15	10.25, 2.39	165.2, 8.35	317.8, 3.58
MNiCoP@C-5	10.51, 0.90	222.6, 2.75	473, 1.68
MCoP@C	10.19, 4.45	322.4, 7.70	702, 1.94
MNiP@C	10.74, 3.32	670.9, 5.20	1241,2.31

Table S4 The ECSA for different samples in 1M KOH

	MNiCoP@C-10	MNiCoP@C-15	MNiCoP@C-5	MCoP@ C	MNiP@ C	NiCo@ C
C(F/g)	62.9	16.5	15.1	11.7	11.4	6.5
ECSA (m²/g)	104.8	27.5	25.2	19.5	18.9	10.8